Construction and Building Materials 115 (2016) 602–617

Contents lists available at ScienceDirect

Construction and Building Materials

journal homepage: www.elsevier.com/locate/conbuildmat

# Organic corrosion inhibitor of triethylenetetramine into chloride contamination concrete by eletro-injection method

C. Xu [a], W.L. Jin [a,b], H.L. Wang [a,*], H.T. Wu [a], N. Huang [a], Z.Y. Li [a], J.H. Mao [b]

[a] Institute of Structural Engineering, Department of Civil Engineering, Zhejiang University, Hangzhou 310058, China
[b] Ningbo Institute of Technology, Zhejiang University, Ningbo 315100, China

## HIGHLIGHTS

- TETA as a corrosion inhibitor was capable of being effectively injected into concrete.
- The TETA concentration around the rebar was adequate to provide corrosion protection.
- Both BIEM and ECE will reduce overall porosity in concrete cover.
- Pore distribution in concrete cover will change after BIEM and ECE treatments.
- Surface strength reduction is more obvious for carbonizated concrete after BIEM.

## ARTICLE INFO

*Article history:*
Received 26 March 2015
Received in revised form 19 April 2016
Accepted 19 April 2016
Available online 28 April 2016

*Keywords:*
Cement
Corrosion inhibitor
Organic inhibitor
Corrosion
Rust

## ABSTRACT

Triethylenetetramine (TETA), a corrosion inhibitor for steel in aqueous media, was introduced into chloride-contaminated concrete specimens using a novel method called bidirectional electromigration rehabilitation (BIEM). An electric field was applied between the embedded steel cathodes and external anodes to inject the corrosion inhibitor from the external electrolytes to the concrete specimens and extract the chloride ions from the concrete cover zone. After treatment, the specimens were drilled to determine the concentration profiles of the corrosion inhibitor, chloride, and hydroxyl ions within the concrete. Effects of variations in the applied current density, duration of electrolysis, water/cement ratio, initial chloride content, and surface carbonation on the concentration profiles of the proposed ions were determined. Electrochemical chloride extraction (ECE) was applied as a control experiment using saturated $Ca(OH)_2$ solution as an external electrolyte. As expected, the chloride content decreased and alkalinity increased after treatment. The concentration of the inhibitor injected around the embedded steel bars was adequate to provide corrosion protection. Concrete strength and pore distribution were measured before and after the electrochemical process was applied. The ability of TETA to inhibit further corrosion after BIEM treatment was also analyzed. The effects of BIEM and ECE were also compared. The results obtained can provide a direction in designing the BIEM process.



## 1. Introduction

Reinforcement corrosion is one of the main causes of deterioration of concrete structures [1,2]. The reinforcing steel in concrete structures exposed in a marine environment or suffering de-icing salt may corrode when the chloride concentration around the steel bar reaches a threshold value, leading to performance degradation or even early structural failure [3,4]. Therefore, the steel must be protected from corrosion to extend the service life of chloride-contaminated reinforcement concrete structures.

Electrochemical methods have been widely applied in rehabilitating existing reinforced concrete structures [5]. Among the electrochemical rehabilitation techniques available, electrochemical chloride extraction (ECE) is the most widely studied and used technique in repairing chloride-contaminated structures. However, this method cannot completely remove the chlorides in the structure and is only a temporary solution because chloride ions tend to come back after treatment is stopped [6–8]. In addition to the removal of chlorides, the use of corrosion inhibitors that can be applied on a concrete cover surface has been suggested to protect reinforcing steel from corrosion [7]. These inhibitors are mostly based on particular amines and alkanolamines or their compounds, which are capable of diffusing considerable distances through a

* Corresponding author.
*E-mail address:* hlwang@zju.edu.cn (H.L. Wang).

http://dx.doi.org/10.1016/j.conbuildmat.2016.04.076
0950-0618/

concrete when applied on the surfaces of the structures by capillary action [9,10]. Although these corrosion inhibitors are effective in preventing reinforcement from corrosion within concrete structures [11,12], the surface-applied inhibitors can hardly penetrate the depth of the embedded steel reinforcement; thus, adequate concentrations are necessary to provide corrosion protection when the concrete cover is too thick or the concrete compaction is too high [13,14]. The possibility of using electrical fields to accelerate their ingress in concrete has been explored. Sawada et al. [15–17] have succeeded in promoting the injection of corrosion inhibitors into carbonated-concrete specimens, significantly reducing the corrosion rates of steel bars.

The present authors [18,19] have explored this kind of method and proposed the remedial technique of bidirectional electromigration rehabilitation (BIEM), through which chloride ($Cl^-$) ions are successively removed along with the injection of inhibitors into the ordinary reinforced-concrete specimens. Triethylenetetramine (TETA), an amine-based corrosion inhibitor, was used during the electrochemical process because of its anticorrosion effectiveness, electrochemical migration capabilities, and environmental friendliness. The effectiveness of electrochemical treatment is influenced by many elements, such as circulated charge and specimen type [20]. Nevertheless, the optimum conditions necessary enhance rates of field-induced injection of the corrosion inhibitor and extraction of $Cl^-$ ions through various types of concrete remains unknown. Therefore, applying the technique appropriately in a field situation is difficult.

Experiments were undertaken with concrete specimens mixed with chloride salt to obtain a deeper understanding of the BIEM method. The concentration profiles of $Cl^-$ ions, hydroxyl ions, and corrosion inhibitor in the concrete cover were measured before and after the electrochemical process. The influence of key factors, such as current density, treatment duration, water/cement ratio, initial chloride content, and surface carbonation, on the electrolysis procedure was investigated. The effects of the BIEM and ECE were also compared.

The concrete strength after BIEM treatment, corrosion inhibitor retention, and long-term corrosion inhibition performance are also important. In the ECE process, the negative ions in the concrete cover migrate toward the anode under electric field action, whereas the positive ions migrate toward the cathode. During this process, hydration products dissolve and new crystals or sediments are generated. Such transformation also occurs in the BIEM; however, the positive ions that migrate toward the cathode are different. Thus, special attention should be given to the positive ions of the corrosion inhibitor. Such transformation could cause changes in the pore distribution and compactness of the concrete cover, which will further affect the surface strength of the concrete. Scholars in China and other parts of the world have performed relevant studies in ECE. New crystals have been generated in the concrete, and changes in the pore size and distribution of the concrete cover were observed after ECE treatment [21–23]. The concrete strength also changed after ECE treatment, with the concrete strength near the anode higher than that close to the cathode [24]. However, with the exception of the above influences, the TETA corrosion inhibitor may have additional effects on the concrete strength and on the pore structures in the BIEM process.

Scholars have studied the effects of self-migration corrosion inhibitor applied to a concrete surface and organic corrosion inhibitor inside a concrete on concrete strength. However, given the difference of specific corrosion inhibitors or application modes, the test results varied. Söylev et al. [25] showed that no significant effect on concrete strength was observed when amine corrosion inhibitor was applied to a concrete surface as a migration corrosion inhibitor. However, Schutter et al. [26] considered that mixing amine corrosion inhibitor with concrete would reduce concrete strength by 10%–30%. Heren et al. [27] showed that the decline in concrete strength was enhanced by an increase in corrosion inhibitor concentration. To date, no scholars have analyzed the influences of the BIEM repair method that is based on electromigration principle on the performance of concrete materials or structures. In practical application of BIEM, special attention should be given to whether or not the material of concrete directly in contact with the electrolyte containing the corrosion inhibitor on the surface will deteriorate and reduce strength under the influence of physical and chemical changes. Material degradation on the concrete surface may destroy its pore characteristic, which will affect its compactness and cause various corrosive mediums to enter the concrete cover. In addition, decline in surface strength caused by material degradation influences the concrete structure and mechanical properties, causing the concrete cover to easily crack.

This study aimed to investigate the effect of control parameters, such as charging parameters, water/cement ratio, chlorine salt concentration, and carbonization, on surface strength. A comparison on the influence of BIEM and ECE on concrete surface strength was studied. Finally, retention of corrosion inhibitor and long-term corrosion inhibition performance after BIEM treatment were also analyzed.

## 2. Technical concepts

The technical concepts of BIEM are illustrated in Fig. 1. An electrical field is applied between the embedded steel as cathode and external anode immersed in the electrolyte that contacts the concrete specimen surface. Under electric field action, the cationic species of the corrosion inhibitor migrate into the concrete cover to the cathode, whereas the chloride ions in the concrete migrate out of the concrete to the anode [18]. The corrosion inhibitor forms a protective film around the embedded steel bars and isolates the corrosive substances, such as chloride and oxygen, when its concentration reaches an adequate value [11]. Moreover, the alkalinity of the pore solutions close to the embedded steel bars is enhanced as a result of the generation of hydroxyl ions at the cathode, which favors steel repassivation.

As described previously, selection of appropriate corrosion inhibitors is the key to the success of the electrochemical treatment. The corrosion inhibitor suitable for BIEM should provide enough corrosion protection under chloride ion condition and should also exist predominantly as cationic species in aqueous media under certain conditions. An amine or alkanolamine-based corrosion inhibitor is a good choice if these requirements are taken into consideration [15–18]. This type of corrosion inhibitor is protonated to an extent governed by the solution pH and the dissociation constants (Ka) of their conjugate acids when dissolved in aqueous solutions, as represented in Eqs. (1) and (2). The degree of hydrolysis of the organic corrosion inhibitors is governed by their dissociation constants ($K_a$) and the solution pH [15]. When the solution pH is equal to $K_a$, the amount of cationic species is equal to that of the molecular species. As the pH value decreases, the number of cationic species increases and the molecular species decrease. The opposite happens when the pH value increases. Given that pH value of the pore solution in the concrete is higher than 12.5, a corrosion inhibitor with large $K_a$ should be chosen to accelerate its injection into the concrete. Triethylenetetramine ($NH_2$-$CH_2CH_2$-$(NHCH_2)_2$-$NH_2$) was chosen as corrosion inhibitor in this study because of its high $K_a$ value and better ability of anticorrosion.

$$RNH_3^+ \leftrightarrow RNH_2 + H^+. \quad (1)$$

$$K_a = \frac{[H^+][RNH_2]}{[RNH_3^+]}. \quad (2)$$

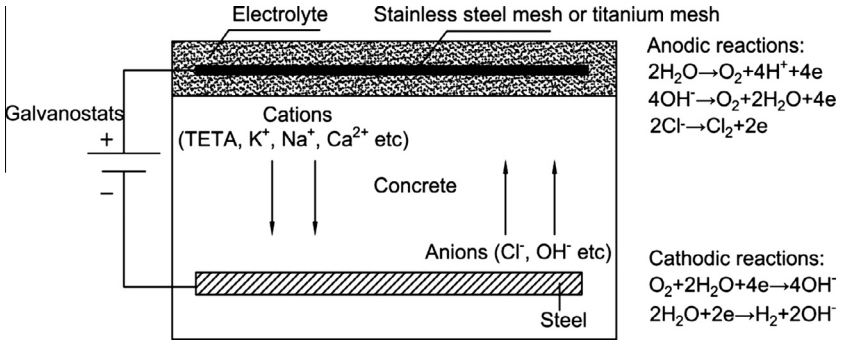


**Fig. 1.** Schematic of technical concept of BIEM.

## 3. Experimental

### 3.1. Specimen preparation

Ordinary Portland cement (OPC) was mixed with NaCl to produce the concrete specimens. The proportions of the concrete mix are shown in Table 1. Specimens with dimensions of 150 mm × 150 mm × 300 mm were cast with two mild steel bars with 12 mm diameter at intervals of 50 mm and cover depths of 40 mm from one face (see Fig. 2). The specimens were demolded after 24 h of casting, and then cured for a minimum period of 3 months to ensure that the cement was properly hydrated. The end surfaces of the steel bar were connected with electric wire and masked with epoxy resin.

### 3.2. Treatment of specimens

The specimen types and their treatment methods are shown in Table 2. For each kind of test, 3 specimens were used to improve the reproducibility.

The specimens were subjected to electrolysis, as illustrated in Fig. 3. The bottom surfaces of the specimens were immersed in an external electrolyte containing TETA (1 mol/L) to a depth of 1 mm, while the side surfaces were sealed with wax to prevent the exchange of ions. The pH of the electrolyte was controlled to about 10 using phosphoric acid [18]. The anodes used were made of Type 316 stainless-steel mesh, whereas the cathodes were steel bars embedded in the specimens. The circuit was then completed and current densities were galvanostatically controlled at 1, 3, or 5 A/m$^2$ of the steel cathode surface area. The periods of treatment were between 7 and 30 d for different specimens. The corrosion of the anodes occurred under high current density; thus, the 316 stainless-steel mesh was changed every 3 d. Saturated $Ca(OH)_2$ solution was used as electrolyte for the specimens subjected to ECE. The pH value of the electrolytes was monitored, and more electrolytes were added whenever the pH value decreases to 7. All chemicals used were analytical-reagent grade, with the exception of TETA, which was >95% pure.

### 3.3. Measurement

#### 3.3.1. Penetration profiles of the corrosion inhibitors, chloride, and hydroxyl ions

The specimens were dried in a shaded area for 24 h after the electrochemical treatments. Samples of concrete powder were obtained every 5 mm along the migration path from different parts of the treated surfaces using a 10 mm drill. The drilling position is shown in Fig. 4. Powders <0.075 mm in size were obtained through a sieve to determine the content of the organic corrosion inhibitor penetrated into the concrete blocks. A 20 mg sample was weighed and wrapped for each sample to measure the corrosion inhibitor content using a Thermo Finnigan flash 1112 EA organic element analyzer. The residual powder under 0.3 mm in diameter was used to determine the $Cl^-$ and $OH^-$ concentrations by titration. A 5 g sample was mixed with 100 ml of deionized water and the resulting mixture was stored for 24 h. The supernatant liquor was used for titration. A Mettler-Toledo T50A automatic potentiometric titrator was used in the experiment. The titrant for the $Cl^-$ titration was 0.01 mol/L of $AgNO_3$ solution and that for $OH^-$ titration was 0.04 mol/L of the HCl solution. A Plug and Play combined silver ring electrode with ceramic frit for argentometric titrations was used for $Cl^-$ titration, whereas Plug and Play combined pH electrode with ceramic frit for direct pH measurements and acid/base titrations in aqueous solutions for $OH^-$ titration.

The long-term performance of TETA corrosion inhibitor after BIEM treatment was investigated by performing the drying and wetting cycle test for half a year, which involved wetting by immersing the samples in 3% NaCl solution for 3 d, followed by natural drying for 3 d. The corrosion inhibitor and chloride content in the test blocks with ECE and BIEM treatment (Concrete type: 1; Mixed NaCl: 3%; Treatment duration: 15 d; Current density: 3 A/m$^2$) and the potential and corrosion rate of untreated blocks were also measured by electrochemical test after six months of exposure.

#### 3.3.2. Surface and compressive strength

Surface strength of the concrete was measured using a 'Limpet' [28,29]. Other related studies were performed in Denmark and USA, leading to a wide range of test configurations and procedures, such as the German Instruments' bond test and James Bond test system that are available in the market.

The pull-off test aims to determine concrete surface strength. The test is also suited to assess bond strength of repairs with the use of a partial coring into the base material. BS1881-207:1992, BSEN1542:1999, and ASTM C1583-04 [30] recommend this pull-off test in quality control and long term monitoring.

The pull-off test method involved bonding a circular steel probe to the surface of a concrete by means of an epoxy resin adhesive, as shown in Fig. 5. A tensile force that slowly increases is applied to the probe. The concrete failed in tension when the tensile strength of the bond strength in the adhesive was greater than the tensile strength of the concrete. The nominal tensile strength of the concrete specimen, called the pull-off strength, was calculated using the area of failure and the force applied at the failure. The compressive strength of the concrete was calculated using Eq. (3) [31].

$$f_{c,c} = 8.65 f_{p,\mathrm{lim}}^{1.29} \quad (3)$$

where $f_{c,c}$ is the conversed-compressive strength of the concrete and $f_{p,lim}$ is the pull-off strength of the concrete.

The blocks were dried naturally for 2 d after electrochemical treatment by BIEM and ECE. Three circular steel probes, each with a diameter of 50 mm, were bound to the surface of a concrete using an epoxy resin adhesive, as shown in Fig. 6. A tensile force that slowly increased with a loading rate below 1 N/s mm$^2$ was then applied to the probes.

#### 3.3.3. Concrete porosity

The pore distribution variation was studied by measuring the concrete porosity. A type 1 concrete parameter was measured before and after ECE and BIEM treatment with different charging times (concrete of type 1, current density: 3 A/m$^2$, 3% NaCl, charging time: 7 d, 15 d, and 30 d) using a mercury porosimeter.

A mercury porosimeter analyzes open pores that are present in a powder or solid block, pore size and pore volume of the fracture, and other parameters by injecting a certain volume of mercury under low pressure and high pressure states

**Table 1**
Mix proportion of concrete.

| Type | Max size of aggregate (mm) | Water (kg/m$^3$) | Cement (kg/m$^3$) | Fine aggregate (kg/m$^3$) | Coarse aggregate (kg/m$^3$) | Mixed NaCl proportion* |
|---|---|---|---|---|---|---|
| 1 | 16 | 220 | 406.4 | 643.1 | 1049.3 | 1%, 3%, 5% |
| 2 | 16 | 220 | 457.6 | 577.6 | 1072.6 | 3% |
| 3 | 16 | 220 | 508.8 | 562.3 | 1044.2 | 3% |

Mixed NaCl proportion*: the ratio of the NaCl mass and the cement mass.

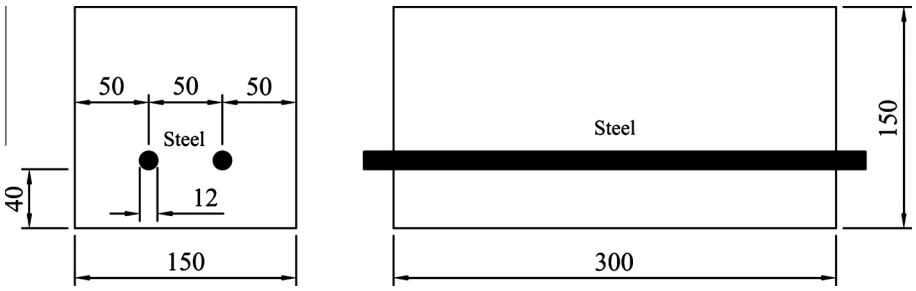


**Fig. 2.** Schematic of the reinforced concrete specimen (dimensions are in mm).

**Table 2**
Specimens types ant their treatment methods for short-term test.

| Specimen | Concrete type | Mixed NaCl | Treatment method | Treatment duration (d) | Current density (A/m$^2$) | Pre-carbonation* |
|---|---|---|---|---|---|---|
| C30-3-0 | 1 | 3% | – | 0 | 0 | No |
| C35-3-0 | 2 | 3% | – | 0 | 0 | No |
| C40-3-0 | 3 | 3% | – | 0 | 0 | No |
| C30-1-0 | 1 | 1% | – | 0 | 0 | No |
| C30-5-0 | 1 | 5% | – | 0 | 0 | No |
| C30-3-B15-1 | 1 | 3% | BIEM | 15 | 1 | No |
| C30-3-B15-3 | 1 | 3% | BIEM | 15 | 3 | No |
| C30-3-B15-5 | 1 | 3% | BIEM | 15 | 5 | No |
| C30-3-B7-3 | 1 | 3% | BIEM | 7 | 3 | No |
| C30-3-B30-3 | 1 | 3% | BIEM | 30 | 3 | No |
| C35-3-B15-3 | 2 | 3% | BIEM | 15 | 3 | No |
| C40-3-B15-3 | 3 | 3% | BIEM | 15 | 3 | No |
| C30-1-B15-3 | 1 | 1% | BIEM | 15 | 3 | No |
| C30-5-B15-3 | 1 | 5% | BIEM | 15 | 3 | No |
| C30-3-C7-3 | 1 | 3% | ECE | 7 | 3 | No |
| C30-3-C15-3 | 1 | 3% | ECE | 15 | 3 | No |
| C30-3-C30-3 | 1 | 3% | ECE | 30 | 3 | No |
| CA30-3-0 | 1 | 3% | – | 0 | 0 | YES |
| CA30-3-B15-3 | 1 | 3% | BIEM | 15 | 3 | YES |
| CA30-3-C15-3 | 1 | 3% | ECE | 15 | 3 | YES |

Pre-carbonation*: pre-carbonation means the surface of the specimen is carbonated by means of accelerated carbonation treatment for 28 d within the concentration of 20% $CO_2$.

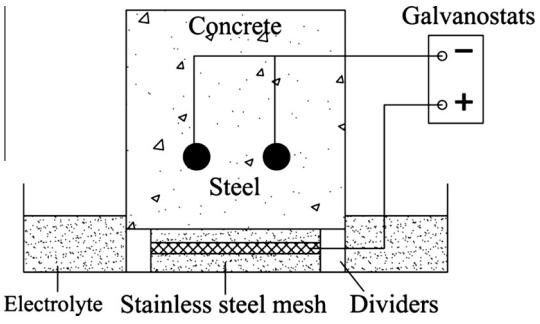


**Fig. 3.** Schematic of experimental arrangement for bidirectional electromigration rehabilitation (BIEM).

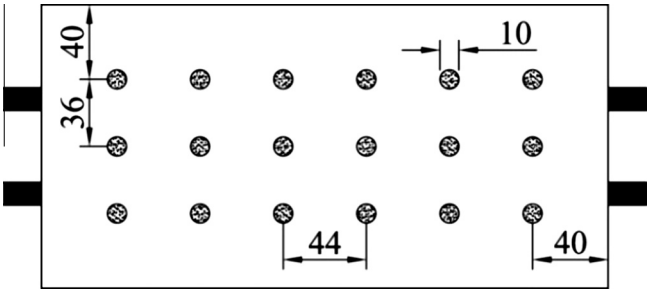


**Fig. 4.** Schematic of the drilling position on the treated surface (dimensions are in mm).

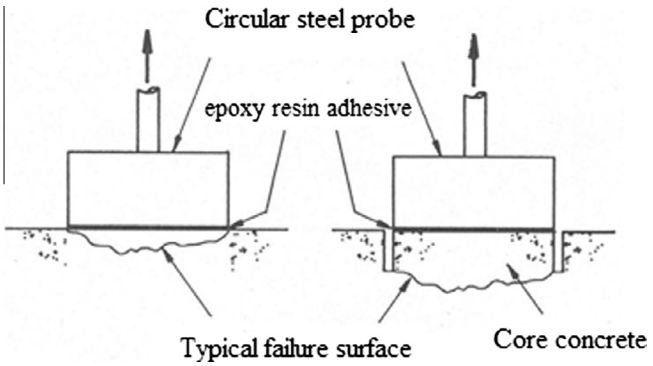


**Fig. 5.** Principle of LIMPET.

[32,33]. This method is effective in measuring pore structure characteristics, and thus, it is extensively applied in the measurement and analysis of microstructures in test samples. Moreover, this method is also suitable for testing large-pore materials.

The mercury quantity entering the pores with different diameters under continuous change of pressure can be measured; thus, the pore diameter distribution can be obtained. The Hg intrusion method has some defects; however, it is still being used because it can measure a great range of pore diameters and offer some degree of visualization of the pore diameter distribution of porous materials (see Table 3).

*3.3.4. Electrochemical measurement*

The half-cell potential and corrosion rate were measured during the drying and wetting cycle test, which was performed for half a year after ECE and BIEM treatment.

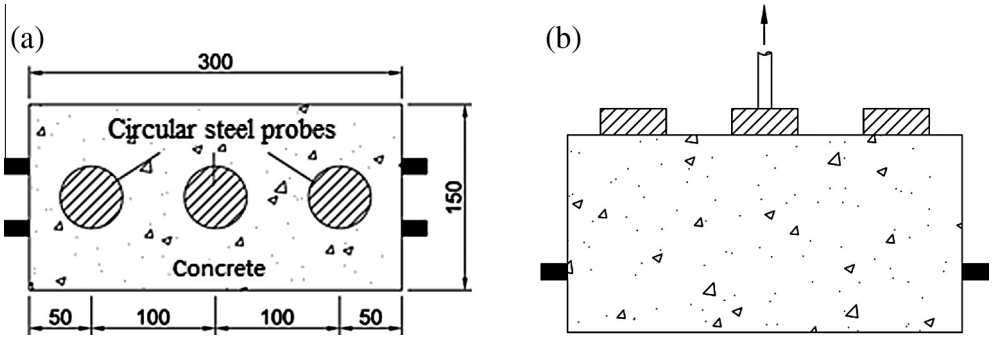


**Fig. 6.** Schematic of pull-off strength test by LIMPET.

Half-cell potential was measured using a standard calomel electrode (SCE). The specimens were kept wet for 0.5 h before measurement to minimize the effect on concrete properties.

Corrosion rate was calculated using linear polarization [34]. Polarization resistance was derived from a gradient of the current to the potential in a linear range. The potential was swept ±15 mV from the corrosion potential at a low scan rate of 0.1 mV $s^{-1}$. The constant corrosion potential was set at 26 mV for active corrosion and 52 mV for passive state. Afterward, the corrosion rate was calculated using Eq. (4):

$$I_{corr} = \frac{B}{R_p} \tag{4}$$

where $I_{corr}$ is the corrosion rate, $B$ is the constant corrosion potential, and $R_P$ is the polarization resistance.

## 4. Results and discussion

### 4.1. Migration properties of the corrosion inhibitors, chloride, and hydroxyl ions

The concentration profiles of the corrosion inhibitor, $Cl^-$, and $OH^-$ ions in the concrete cover and the value of $OH^-/Cl^-$ and TETA/$Cl^-$ played significant roles in determining the probability of steel corrosion. These parameters are important in evaluating the effectiveness of the electrochemical remedial techniques. Therefore, they were measured in the experiment using a given current density, treatment duration, water/cement ratio (w/c), mixed $Cl^-$ content, or surface carbonation as the control parameters. Moreover, the effects of ECE and BIEM were also compared.

#### 4.1.1. Influence of current density

As illustrated in Fig. 7(a)–(c), the concentration profiles of $Cl^-$, $OH^-$, and TETA were modified depending on the applied current densities. A type 1 concrete with 3% NaCl (vs cement mass) was used in this experiment and the treatment time was 15 d.

The residual $Cl^-$ concentration in the specimens decreased with an increase in current density. The increase in current density increased the effectiveness of $Cl^-$ extraction as the circuit charge was increased. However, the residual $Cl^-$ in the outermost layer was higher than that in the untreated specimens when the current density was <3 A/$m^2$. This means that the applied electric field was not sufficient to completely remove the $Cl^-$ ions, resulting in the accumulation of $Cl^-$ in the specimens' outer layer. The removal efficiency of $Cl^-$ is defined as the ratio of the difference between the initial $Cl^-$ concentration and the residual $Cl^-$ concentration to the value of the initial $Cl^-$ concentration in the vicinity of the embedded steel. This removal efficiency was used to evaluate the effect of $Cl^-$ extraction during the electrochemical process. As indicated in Fig. 7(a), the removal efficiency of $Cl^-$ increased from 21% to 65% and finally to 78% when the current density was changed from 1 A/$m^2$ to 3 A/$m^2$ and then to 5 A/$m^2$. These results indicate that when the current density was increased to a certain level, it was difficult to increase the extraction effectiveness of $Cl^-$ by means of increasing the current density.

The change in the water-soluble $OH^-$ concentration was in accordance with the alkalinity change in the concrete. As shown in Fig. 7(b), the alkalinity decreased from the inside to the outside, owing to the presence of $CO_2$ and $H_2O$ in the atmosphere. The alkalinity of the concrete cover increased as the treatment progressed because of the $OH^-$ ions that were generated during the cathodic reaction and increasing as the enhancement of current density. The $OH^-$ concentration of the concrete increased to 21% under the applied electric field with a current density of 1 A/$m^2$; however, the alkalinity of the outer-layer concrete only exhibited a slight increase. Nevertheless, when the current density was increased to 3 A/$m^2$ and 5 A/$m^2$, the alkalinity of the outer-layer concrete was significantly increased and the value of $[OH^-]/[Cl^-]$ around steel was increased from 7.5 to 30, which is far higher than the corrosion threshold value 0.1–1 [35]. As a result, the possibility of steel corrosion was reduced and the ability of a structure to resist carbonation was improved.

Migration of a corrosion inhibitor was also affected by the current density, as illustrated in Fig. 7(c). The concentration of TETA within the first 20 mm from the embedded steel bars was almost the same in a relatively low range; however, the concentration increased in the outer 20 mm layer. The concentration of TETA in the specimens also increased with an increase in current density. Organic corrosion inhibitors were ineffective in preventing steel corrosion when their concentrations were too low [36]. The corrosion inhibitors can provide adequate protection for reinforcement only when the concentration of TETA was higher than that of the chloride ions in the pore solution [18,37]. The concentration of the inhibitors that penetrated the surface of the steel increased by 176% when the current density was increased from 1 A/$m^2$ to 3 A/$m^2$. However, this increase was only 16% when the current density was varied from 3 A/$m^2$ to 5 A/$m^2$.

The relationship between the ratios of the different constituents and current density is shown in Fig. 7(d). The minimum ratio of the concentration of a corrosion inhibitor to that of $Cl^-$ ions when the inhibitor is able to provide effective protection for reinforcement is defined as the effective value of the corrosion inhibitor. The effective value was assumed to be 1 in most cases [18,37]. When the

**Table 3**
Chloride content on the surface of reinforcement (mol/g).

| Treatment type | Chloride content | |
|---|---|---|
| | Before cycle test | After cycle test |
| Untreated | 0.60 | 0.77 |
| ECE | 0.23 | 0.32 |
| BIEM | 0.15 | 0.27 |

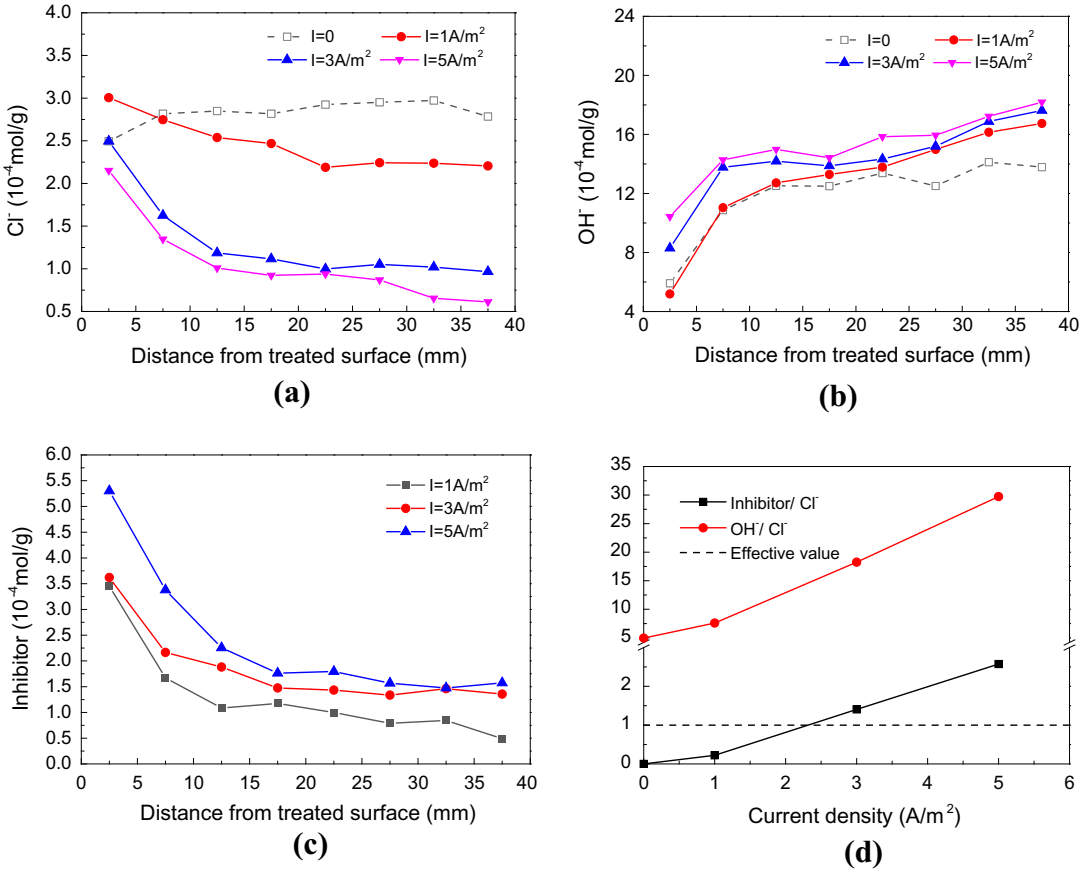


**Fig. 7.** Concentration profiles/ratios in specimens after BIEM for different current densities (Concrete type: 1; Mixed NaCl: 3%; Treatment duration: 15 d; Current density: 0, 1, 3, 5 A/m$^2$). (a) Concentration profiles of $Cl^-$ (by weight of cement). (b) Concentration profiles of $OH^-$ (by weight of cement). (c) Concentration profiles of inhibitor (by weight of cement). (d) Ratios of proposed constituents close to the steel reinforcement.

current density reached 3 A/m$^2$, the (TETA)/$Cl^-$ ratio exceeded 1. The $OH^-$/$Cl^-$ ratio near the steel also increased with an increase in the current density, contributing to more effective corrosion protection for reinforcement [38,39]. The increase in current density played a positive role in the increase in concentrations of TETA and $OH^-$ and the decrease in $Cl^-$, however, the effect was limited. Thus, it is significant to set a proper current density accordingly.

*4.1.2. Influence of treatment duration*

Fig. 8(a)–(c) show the variations in concentrations of TETA, $Cl^-$, and $OH^-$ ions that were plotted as a function of treatment time. A type 1 concrete with 3% NaCl was used in this experiment and the current density was maintained at 3 A/m$^2$.

The residual $Cl^-$ was uniformly distributed in the range of 20 mm at the front of the embedded steel bars and it increased gradually to the treated surface Fig. 8(a). More $Cl^-$ ions were extracted as the treatment duration was increased. Around 38% of $Cl^-$ ions were removed in the layer close to the steel bars after 7 d. When the treatment time was increased to 15 d and 30 d, the percentage of $Cl^-$ ions that were removed reached 65% and 85%, respectively. The concentration of $Cl^-$ in the outermost layer exceeded the initial concentration by 35% after 7 days of treatment because the $Cl^-$ migrated to the anode under the influence of the applied electrical field. The concentration difference of $Cl^-$ between the inner part and the outer part of the specimen was enhanced, leading to the acceleration of counter-migration of $Cl^-$ to the reinforcement after treatment [40].

The distribution tendency of $OH^-$ in the concrete cover zone remained almost the same after BIEM treatment with a small decrease in the concentration difference, as shown in Fig. 8(b). The alkalinity increased with increasing treatment time. An increase in the water-soluble $OH^-$ around the steel was observed, which were 14%, 28%, and 35% after 7, 15, and 30 d, respectively. A slow increase in alkalinity was observed when the treatment duration was prolonged.

The concentration of a corrosion inhibitor in a concrete cover zone increased with an increase in treatment time, as shown in Fig. 8(c). The concentration of TETA in the layer that was close to the surface kept increasing as treatment time progressed. However, the trend in concentration enhancement was different in the vicinity of the embedded steel bars. The concentration of TETA that was near the reinforcement increased by 44% from 7 d to 15 d using the electrolysis procedure, while it increased by only 20% from 15 d to 30 d. This was attributed to the continuous generation of $OH^-$ during cathodic reaction that increased the alkalinity of the concrete. As a result, the cationic species of TETA in the concrete pore solution was reduced with an increase in pH value, which made it difficult for the corrosion inhibitor to migrate into the concrete cover zone [15].

The relationship between the ratios of the different constituents and the treatment time is shown in Fig. 8(d). The value of the TETA/$Cl^-$ ratio after the specimen was treated for 15 d exceeded one, suggesting an effective prevention of steel corrosion. The ratio of $OH^-$ to $Cl^-$ was also increased with an increase in treatment time, which supported the repassivation of the corroded steel bars.

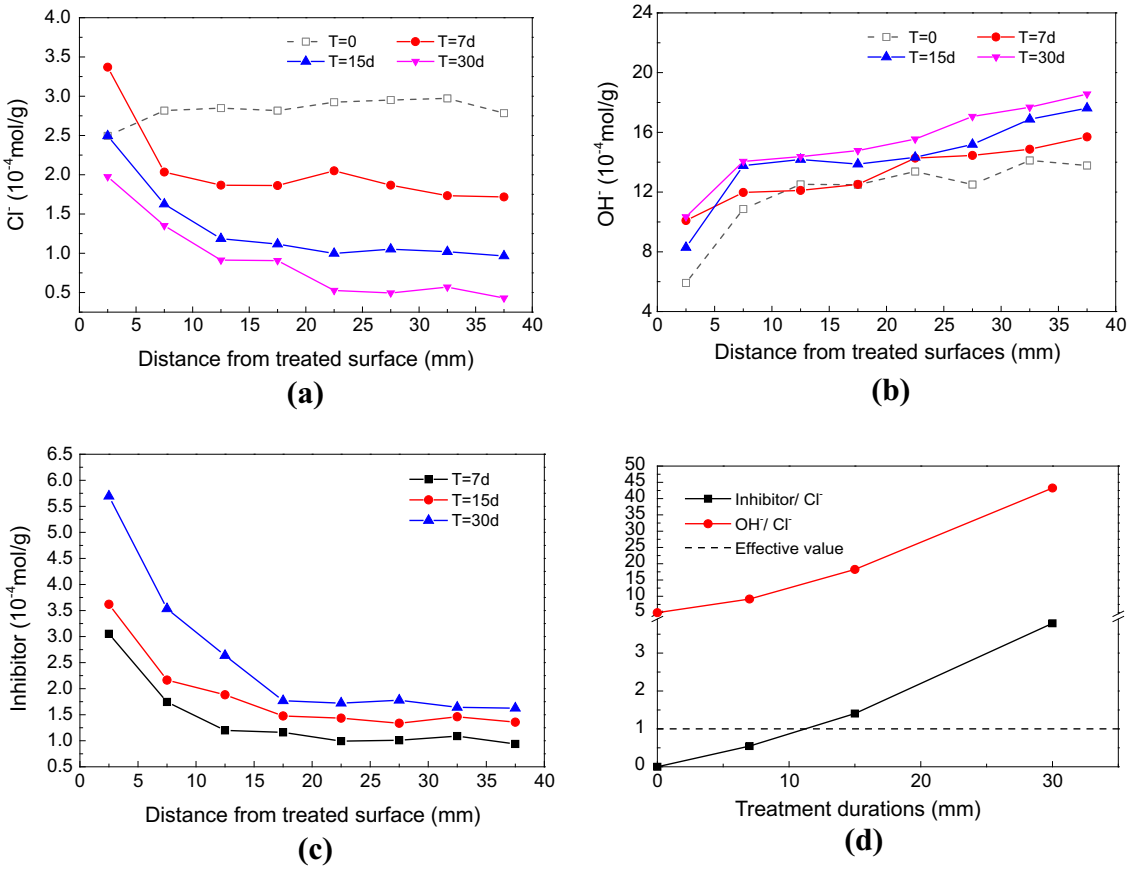


**Fig. 8.** Concentration profiles/ratios in specimens after BIEM for different treatment durations (Concrete type: 1; Mixed NaCl: 3%; Treatment duration: 0, 7, 15, 30 d; Current density: 3 A/m$^2$). (a) Concentration profiles of $Cl^-$ (by weight of cement). (b) Concentration profiles of $OH^-$ (by weight of cement). (c) Concentration profiles of inhibitor (by weight of cement). (d) Ratios of proposed constituents close to the steel reinforcement.

*4.1.3. Influence of water/cement ratio*

The concentration profiles of $Cl^-$, $OH^-$, and TETA in the specimens containing different water (w)/cement (c) ratios are shown in Fig. 9(a)–(c). Concrete of types 1, 2, and 3 were used in this experiment. Each concrete was mixed with 3% of NaCl. The current density used was 3 A/m$^2$ and the treatment lasted for 15 d.

As illustrated in Fig. 9(a), the residual concentration of the $Cl^-$ ions decreased as the w/c ratio increased. A higher w/c ratio caused a higher porosity and lower compactness. As a result, the resistance to $Cl^-$ migration was reduced and the diffusion coefficient of $Cl^-$ was increased [41]. However, the residual concentration of the $Cl^-$ in the outermost layer did not vary significantly with changes in the w/c ratio.

The overall concentration of the $OH^-$ ions increased with increasing w/c ratio, as shown in Fig. 9(b). A higher initial $OH^-$ concentration was observed for the concrete with higher w/c ratio. The concentration of the $OH^-$ ions increased by a small amount when the w/c ratio was decreased from 0.48 to 0.43. However, there was a significant increase in the $OH^-$ concentration when the w/c ratio was decreased from 0.54 to 0.48.

As indicated in Fig. 9(c), the concentration of TETA in the front steel bars was enhanced with increasing w/c ratios. Nevertheless, the TETA concentration was maintained in the outermost layer that was close to the surface even with the use of different w/c ratios. As mentioned above, the concrete with higher w/c ratio had lower compactness and alkalinity, leading to a higher concentration of cationic TETA in the pore solution. Hence, the efficiency of TETA migration was higher in concretes with higher w/c ratio.

The ratios of the different constituents in the concrete cover are illustrated in Fig. 9(d). When w/c was greater than 0.48, The TETA/$Cl^-$ ratio was greater than the effective value. However, the TETA/$Cl^-$ ratio was less than the effective value when the w/c ratio was equal to 0.43, in which the current density and treatment time were extended accordingly. The w/c ratio had little effect on the ratio of $OH^-$ and $Cl^-$ in the BIEM process.

*4.1.4. Influence of initial chloride content*

The concentration profiles of $Cl^-$, $OH^-$, and TETA in the specimens that were mixed with different initial quantities of NaCl after BIEM treatment are shown in Fig. 10(a)–(c). Type 1 concrete that was mixed with NaCl at three different concentrations corresponding to 1%, 3%, and 5% was used to manufacture these specimens. The circuits were galvanostatically controlled at 3 A/m$^2$ for a period of 15 d.

As illustrated in Fig. 10(a), the extraction efficiency of $Cl^-$ in the concrete increased with the initial chloride concentration. The proportion of the extracted $Cl^-$ in the front steel bars were about 44%, 65%, and 78% for the specimens with 1%, 3%, and 5% of NaCl, respectively. These results indicate that the efficiency of BIEM was higher for those structures under heavy chloride attack.

The concentration of the $OH^-$ ions in the concrete cover kept increasing from the outside to the inside after treatment [Fig. 10 (b)]. The overall concentration of $OH^-$ was lower in the specimen that was mixed with 3% NaCl. However, the alkalinity of the specimen that was mixed with 5% NaCl was almost highest especially for that near the embedded steel bars.

There was no significant correlation observed between the migration of TETA and the initial concentration of NaCl that was mixed in the concrete. It implies that the initial chloride content

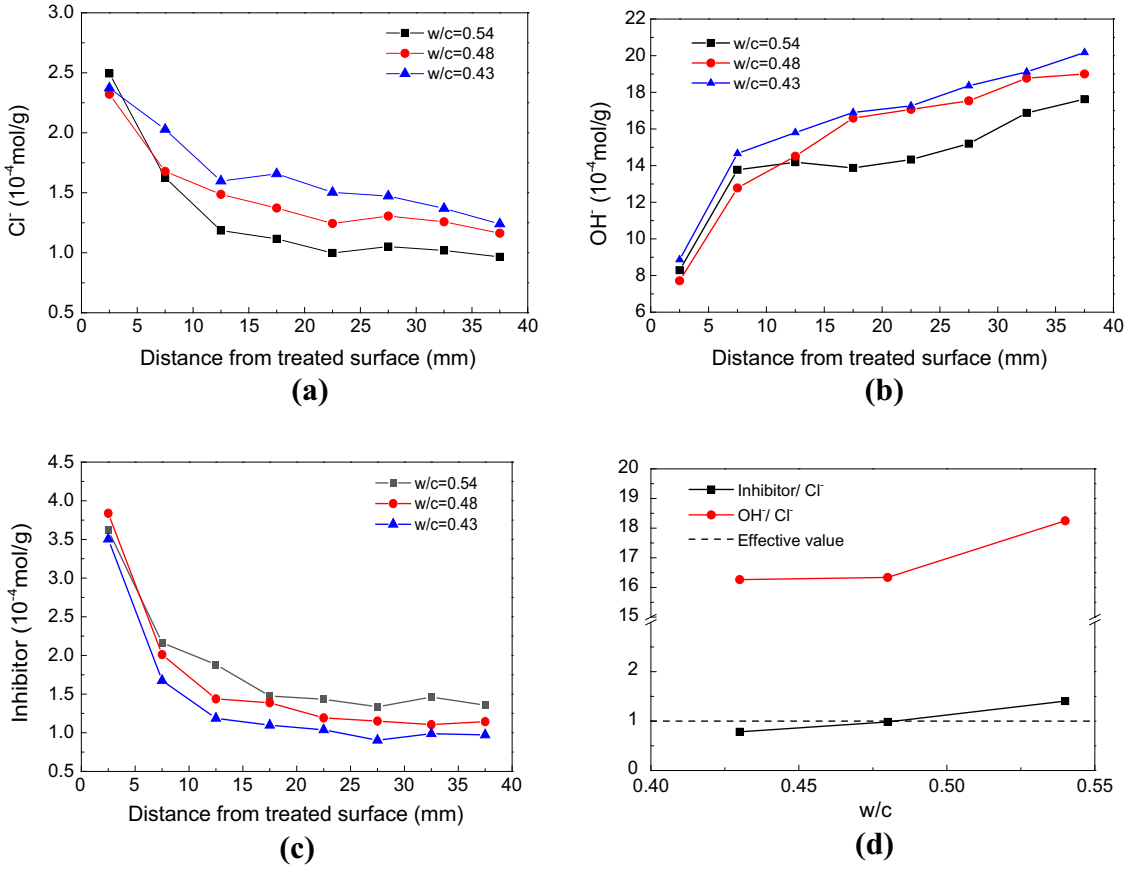


**Fig. 9.** Concentration profiles/ratios in specimens after BIEM for different water/cement ratios (Concrete type: 1, 2, 3; Mixed NaCl: 3%; Treatment duration: 15 d; Current density: 3 A/m$^2$). (a) Concentration profiles of $Cl^-$ (by weight of cement). (b) Concentration profiles of $OH^-$ (by weight of cement). (c) Concentration profiles of inhibitor (by weight of cement). (d) Ratios of proposed constituents close to the steel reinforcement.

of the concrete had little influence on the efficiency of TETA ingression.

The $OH^-/Cl^-$ and $TETA/Cl^-$ ratios were higher in the specimen with 1% NaCl after the electrochemical process was performed; this was due to the low initial concentration of $Cl^-$. This results suggested that the bidirectional electromigration rehabilitation may have better effect on concrete structures with less $Cl^-$ concentration. The $OH^-/Cl^-$ and $TETA/Cl^-$ ratios between the specimens with 3% and 5% NaCl did not exhibit significant difference. Nevertheless, the process played an active role in preventing the reinforcement from corrosion since the all of the ratios of the corrosion inhibitor to chloride ions exceeded one, as shown in Fig. 10(d).

*4.1.5. Influence of different electrolysis*

The residual concentration profiles of $Cl^-$ and $OH^-$ after BIEM and ECE are illustrated in Fig. 11(a) and (b). The specimens in this experiment were cast with type 1 concrete with 3% NaCl. The current density applied was 3 A/m$^2$.

The residual $Cl^-$ ion distributions were different after performing two processes of BIEM and ECE. The overall concentration of the $Cl^-$ in the whole concrete cover was reduced evenly. By contrast, the residual concentration of $Cl^-$ in the specimens' outer layer was higher than in the inner layer after the conduct of BIEM. One possible explanation for this occurrence is the accumulation of several cationic TETA species in the specimens' outer layers where the cations were combined with the $Cl^-$ ions; this led to a difficulty in the extraction of $Cl^-$. The residual $Cl^-$ concentrations around the steel were equal after performing BIEM and ECE for 7 d. When the treatment duration extended to 15 d and 30 d, the effect of BIEM was better than ECE in terms of $Cl^-$ removal. This suggested that BIEM exhibited higher $Cl^-$ removal efficiency than ECE. It is suggested that short-time ECE be performed after BIEM treatment to extract $Cl^-$ better in the overall concrete cover zone, especially in the outer layer.

The distribution trend of alkalinity in the specimens after performing ECE was in accordance with that after BIEM treatment, as shown in Fig. 11(c). However, the level of the concentration enhancement of water-soluble $OH^-$ after ECE was higher than that after performing BIEM.

BIEM exhibited a better effect in increasing the ratio of $OH^-$ to $Cl^-$ than equal-time ECE, as illustrated in Fig. 11(c).

*4.1.6. Influence of surface carbonation*

The average carbonation depth of the specimens that experienced pre-carbonation was 13.7 mm; this was measured by the phenolphthalein test. The carbonated and non-carbonated specimens were all subjected to ECE and BIEM at a current density of 3 A/m$^2$ for a period of 15 d. The concentrations of $Cl^-$, $OH^-$, and TETA in the concrete cover after treatment were plotted in Fig. 12(a)–(c).

The distribution trends of residual concentration of $Cl^-$ in the surface-carbonated specimen decreased from the outside to the inside according with that in non-carbonated specimen. In the 20 mm that was close to the embedded steel bars, the residual $Cl^-$ concentration was higher in the carbonated specimen than in the non-carbonated specimen after performing BIEM. For ECE, however, the $Cl^-$ extraction efficiency was higher in the

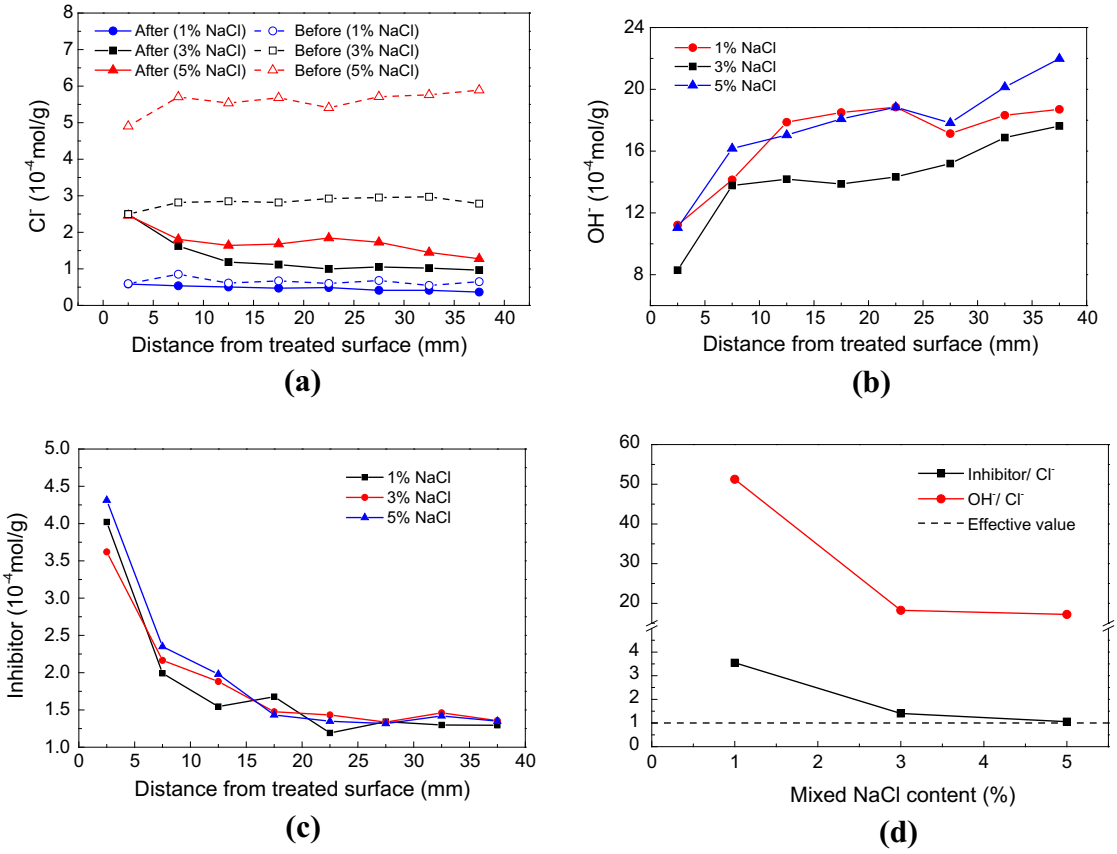


**Fig. 10.** Concentration profiles/ratios in specimens after BIEM for different mixed NaCl contents (Concrete type: 1; Mixed NaCl: 1, 3, 5%; Treatment duration: 15 d; Current density: 3 A/m$^2$). (a) Concentration profiles of $Cl^-$ (by weight of cement). (b) Concentration profiles of $OH^-$ (by weight of cement). (c) Concentration profiles of inhibitor (by weight of cement). (d) Ratios of proposed constituents close to the steel reinforcement.

carbonated specimen than that in the non-carbonated specimen. In general, the effect of ECE was better than BIEM on the removal of $Cl^-$ ions within the concrete cover zone.

The alkalinity of concrete in the distance that was 15 mm near the treated surface decreased sharply, which was influenced by the presence of $CO_2$ and $H_2O$. The increase in the $OH^-$ concentration after BIEM was substantial in the carbonated-surface specimen, especially the first 15 mm that was close to the treated surface. The result in terms of increase in alkalinity after performing ECE was different between carbonated and non-carbonated specimens. The increase in alkalinity that was caused by BIEM was higher in the surface-carbonated specimen than in non-carbonated specimen.

The efficiency of TETA migration was better in the carbonated specimen than those in the non-carbonated specimen, especially in the outer part close to the concrete surface which had been carbonated. In the layer close to the reinforcement, the concentration of inhibitors in the surface-carbonated specimen was 33% higher than that in the non-carbonated specimen. This phenomenon was attributed to the decrease in alkalinity that was close to the concrete surface, leading to a rise in number of cationic TETA species. Therefore, the migrating ability of TETA was improved. However, the inner part of the specimen was not influenced by carbonation; thus, the increase of TETA was limited.

### 4.2. Concrete strength variation after BIEM and ECE treatment

As shown in Fig. 13, the surface strength of the concrete sample did not decrease after ECE treatment; instead, it was greatly enhanced. The reason might be that after concrete sample experiences ECE treatment, the calcium ions in the pore solution were bound with the negative ions that were excreted from the concrete to form some insoluble hydration products which can fill the pores to some extent. As a result, the porosity near the surface of the concrete cover decreased and the material then became more compact [42].

The influence of BIEM on the surface strength in the concrete cover was contrary with that of ECE. The surface strength in the concrete cover of the sample decreased after BIEM treatment. The different effects of these two technologies may be related to the different kinds of their electrolyte. The TETA corrosion inhibitor may damage ingredients or material structures of concrete and such effect may be related to the concentration of the corrosion inhibitors in the concrete.

#### 4.2.1. Influence of current density on concrete strength after BIEM treatment

In order to examine the effect of electric current density, we performed tests for the same type (concrete of Type 1, 3% NaCl) and the same charging time (15 days) but different current densities to evaluate the variation of concrete surface strength. Fig. 14 shows the variation of concrete surface strength after BIEM treatment as a function of electric current densities.

The surface strength of the concrete sample decreased by varying degrees after the BIEM treatment. It shows that TETA corrosion inhibitor caused negative effects on the surface strength of the concrete. Fig. 14 also shows that the reduction degree of the surface strength after the BIEM treatment with different electric current density. With the electric current density increased, the surface strength presented a decrease trend. When the electric current density was 1 A/m$^2$ or 3 A/m$^2$, the pull-out strength was decreased by ~18–19% and the converted compressive strength was reduced

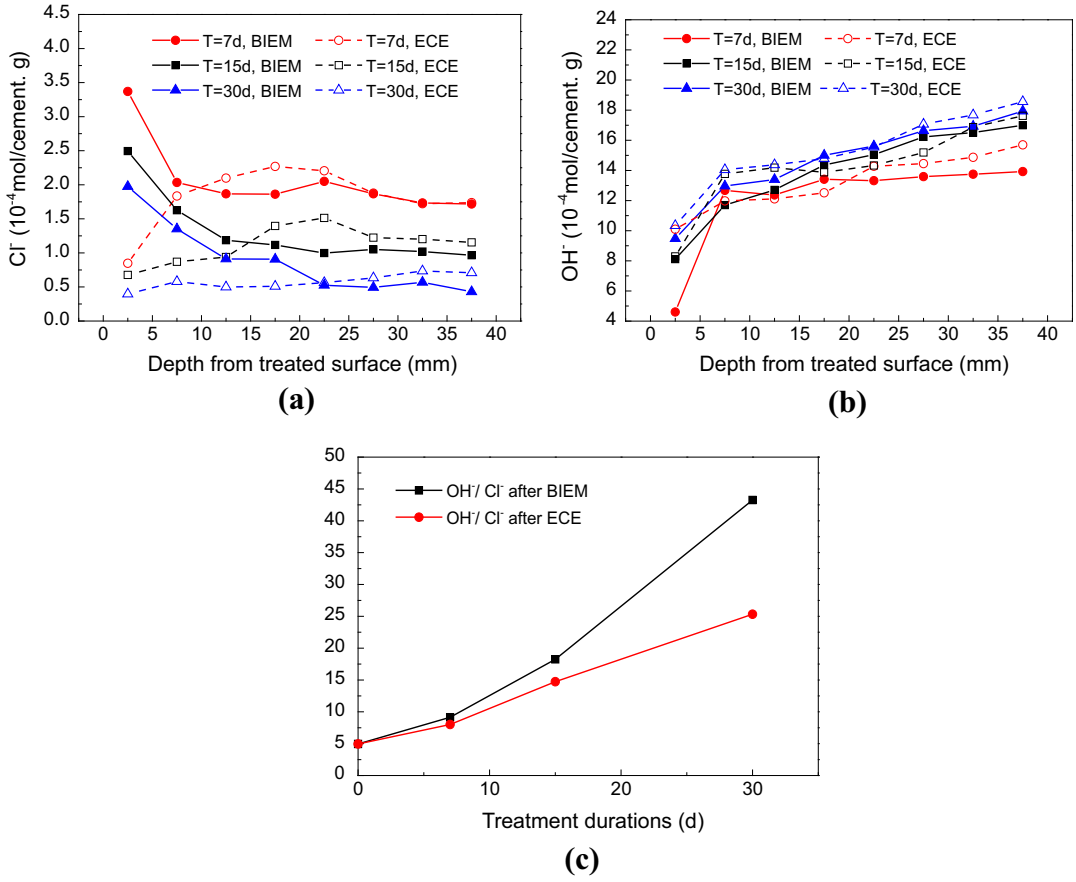


**Fig. 11.** Concentration profiles/ratios in specimens after electrochemical treatments of different kinds (Concrete type: 1; Mixed NaCl: 3%; Treatment method: BIEM and ECE; Treatment duration: 7, 15, 30 d; Current density: 3 A/m$^2$). (a) Concentration profiles of $Cl^-$. (b) Concentration profiles of $OH^-$. (c) Ratios of proposed constituents close to the steel reinforcement.

by ~22%–24%. When the electric current density was increased to 5 A/m$^2$, the surface strength reduced sharply. The pull-out strength decreased by 43% and the converted compressive strength was reduced by 51%.

Therefore, when the BIEM method is adopted for repair, the electric current should be strictly controlled. Increase in electric current will increase migration rate of ions, and enhance the repair effect to some degree, but excessively high electric current will cause adverse effects on reinforcement performance [43]. Moreover, surface strength of the concrete structure will greatly decrease, and craze may even be generated on the surface.

*4.2.2. Influence of charging time on concrete strength after BIEM treatment*

Similarly, the samples were treated by BIEM with different charging time. The test used sample type (concrete of category 1, 3% NaCl) and electric current density (3 A/m$^2$) constants, and tracked the variation of concrete surface strength after BIEM treatment with different durations. The variation of surface strength with charging duration was deduced based on the test results shown in Fig. 15.

The test results show that the surface strength of the sample decreases with increase in charging time, almost in a linear relation. Charging for seven days has a minimal effect on surface strength. In particular, the pull-out strength was decreased by 12%, and the converted compressive strength was reduced by 15%. However, after charging for 30 days, the surface strength of the sample greatly decreased, i.e., the pull-out strength decreased by 44% and the converted compressive strength was reduced by 52%. Moreover, in the practical application of BIEM technology, charging time should be reasonably controlled because extended charging time will greatly damage the sample surface.

*4.2.3. Influence of water–cement ratio on concrete strength after BIEM treatment*

BIEM treatment under the same conditions was conducted for concrete samples with different mix proportions (concrete of categories 1, 2, and 3; 3% NaCl) with electric current density of 3 A/m$^2$ and charging time of 15 days. Fig. 16 shows the surface strength variation before and after treatment of samples.

The surface strength of concrete samples with different water–cement ratios decreased after BIEM treatment. The reduction degree increased slightly when water–cement ratio increased, i.e., the change rate of pull-out strength was approximately −20% to 16%, and the change rate of converted compressive strength was approximately −24% to 20%.

*4.2.4. Influence of initial chloride content on concrete strength after BIEM treatment*

Similarly, BIEM test under the same conditions was conducted for concrete samples of different initial chloride contents (concrete of category 1, NaCl contents of 1%, 3%, and 5%) with electric current density of 3 A/m$^2$ and charging time of 15 days. Fig. 17 shows the surface strength variation before and after treatment of samples.

According to Fig. 17, the surface strength of concrete samples with different chloride contents decreased after BIEM treatment. When the NaCl content was 5% of the cement mass, the change rate of surface strength was almost the same as when the NaCl content was 3%. The pull-out strength decreased by approximately 18–19%, and the converted compressive strength decreased by

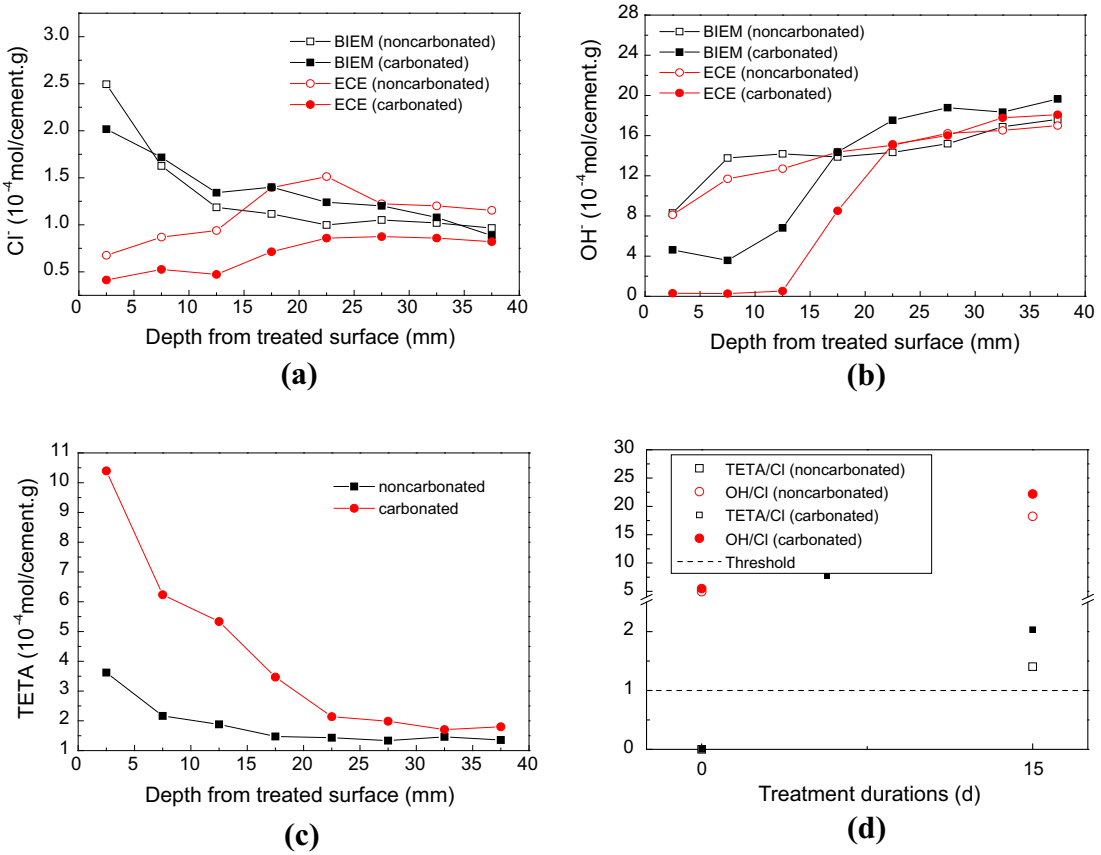


**Fig. 12.** Concentration profiles/ratios in specimens with carbonated and non-carbonated after BIEM for different surfaces (Concrete type: 1; Mixed NaCl: 3%; Treatment method: BIEM and ECE; Treatment duration: 15 d; Current density: 3 A/m$^2$). (a) Concentration profiles of $Cl^-$. (b) Concentration profiles of $OH^-$. (c) Concentration profiles of TETA. (d) Ratios of proposed constituents in front of the steel reinforcement.

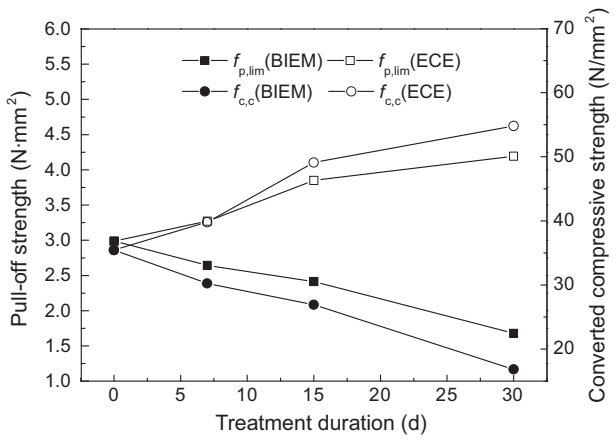


**Fig. 13.** Concrete strength for specimens after BIEM and ECE treatment (Concrete type: 1; Mixed NaCl: 3%; Treatment method: BIEM and ECE; Treatment duration: 0, 7, 15, 30 d; Current density: 3 A/m$^2$).

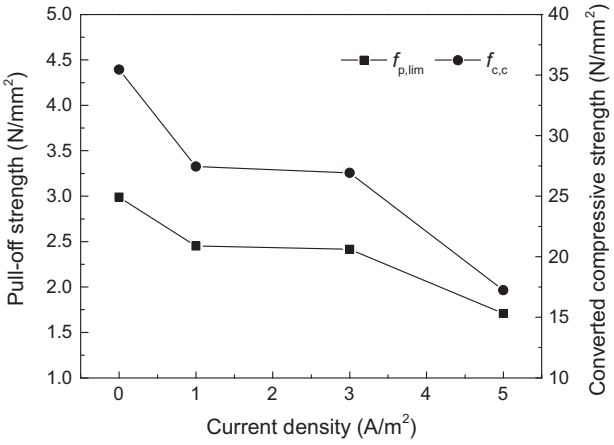


**Fig. 14.** Concrete strength variation for specimens under different current density after BIEM treatment (Concrete type: 1; Mixed NaCl: 3%; Treatment duration: 15 d; Current density: 1, 3, 5 A/m$^2$).

approximately 23–24%. However, when the NaCl content decreased to 1%, the reduction range of surface strength was high, i.e., the reduction rates of pull-out strength and converted compressive strength reached 29% and 35%, respectively. Such results show that for concrete with low chloride concentration, BIEM repair technology will cause greater damage to the concrete surface; thus, caution should be exerted in practical application.

#### *4.2.5. Influence of carbonation on concrete strength after BIEM treatment*

Four groups of samples with the same mix proportion (concrete of type 1, 3% NaCl) were selected, and placed into the carbonation tank for accelerated carbonation test. The carbonation depth of the sample after 28 days of carbonation was approximately 13.7 mm. Then, BIEM test was conducted for samples that underwent and did not undergo carbonation, with an electric current density of 3 A/m$^2$ and charging time of 15 days.

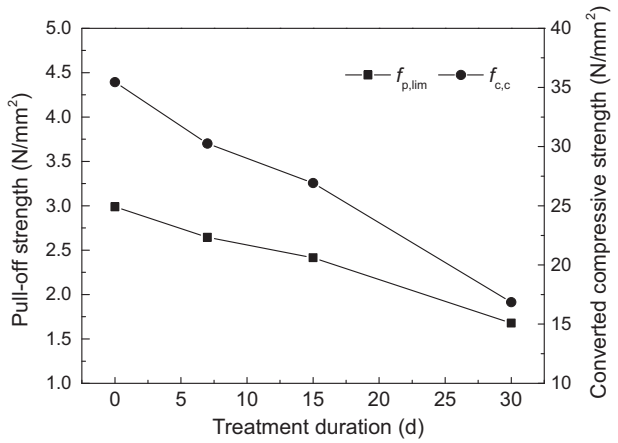


**Fig. 15.** Concrete strength variation for specimens under different charging time after BIEM treatment (Concrete type: 1; Mixed NaCl: 3%; Treatment duration: 0, 7, 15, 30 d; Current density: 3 A/m$^2$).

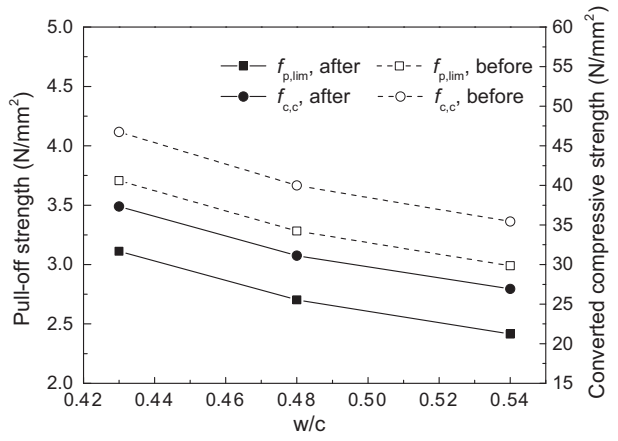


**Fig. 16.** Concrete strength variation for specimens with different water-cement-ratio after BIEM treatment (Concrete type: 1, 2, 3; Mixed NaCl: 3%; Treatment duration: 15 d; Current density: 3 A/m$^2$).

According to the test results shown in Fig. 18, the concrete surface strength increased to 35% after carbonation. After BIEM treatment, the surface strength decreased, and the reduction range increased with time. The reduction rate of surface strength of carbonation samples was greater than non-carbonate samples under the same conditions. It was possibly because the pH value on the surface of carbonate samples was low. However, the test result also shows that the absolute value of surface strength of carbonized sample after carbonation treatment was greater than non-carbonate samples after treatment under the same conditions. Note that carbonation will reduce the alkalinity in concrete cover, which may cause depassivation and corrosion to the reinforcement. Thus, the concrete cover will crack and even spall. However, BIEM will induce the corrosion inhibitor to migrate toward the reinforcement, and increase the pH value of the areas near the reinforcement and the entire concrete cover through cathodic reactions. This process is beneficial for eliminating the adverse effect caused by carbonation. Moreover, carbonation will enhance compactness of the concrete, and increase surface strength of the sample. This effect can offset the effect of BIEM on surface strength of the structure to some extent. For a concrete structure that undergoes severe chloride attack and requires repair, the exposure time is often long and carbonation may occur on the surface. In this case, application of BIEM technology will be more advantageous.

### 4.3. Concrete porosity variation after electrochemical repair

#### 4.3.1. Pore distribution variation after BIEM treatment

After BIEM treatment, porosity and pore distribution in the concrete cover significant changed. According to Fig. 19, porosity decreased when charging time increased, and porosity of concrete was higher around the cathode than around the anode.

Wu [44] characterized the pore diameters into the following gradings (1973): harmless to the pore (<20 nm), little harmful to the pore (20–100 nm), harmful pore (100–200 nm), and great harmful pore (>200 nm). According to this characterization, this paper conducts an in-depth analysis on the pore distribution in concrete cover before and after BIEM treatment. Fig. 20 (a) and (b) show the pore distributions of concretes near the anode and cathode, respectively. The figures show that after BIEM treatment, the porosity of large pores including pore with great harmful, harmful pore and little harmful pore decreased. As for harmless pore below 20 nm, the porosity increased. In general, porosity near the anode was lower than that near the cathode.

The above mentioned analysis shows that BIEM has a positive effect on pore distribution in the concrete cover. The decrease in large pores and increase in small pores is because some hydration

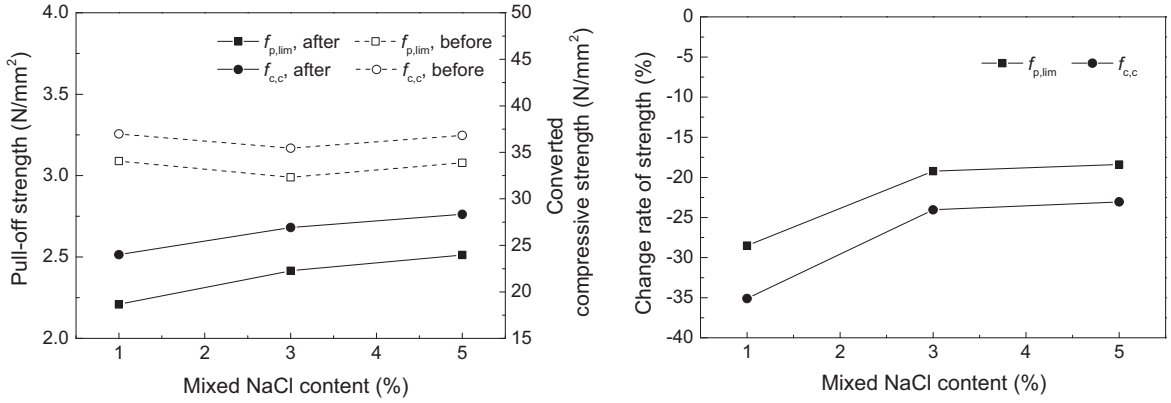


(a) Surface and compressive strength

(b) Change rates of surface and compressive strength

**Fig. 17.** Concrete strength variation for specimens with different initial chloride content after BIEM treatment (Concrete type: 1; Mixed NaCl: 1, 3, 5%; Treatment duration: 15 d; Current density: 3 A/m$^2$).

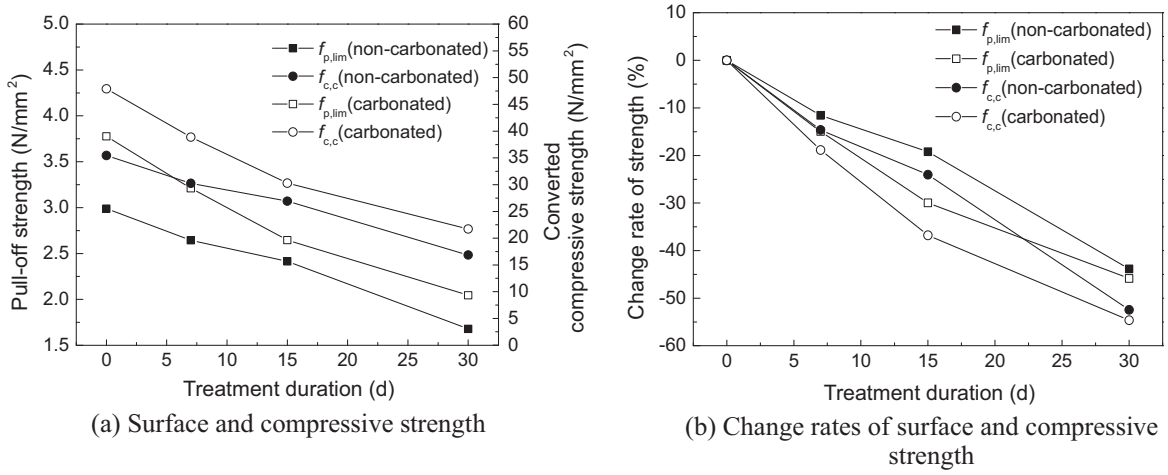


**Fig. 18.** Concrete strength variation for specimens with carbonated and non-carbonated after BIEM treatment (Concrete type: 1; Mixed NaCl: 3%; Treatment duration: 15 d; Current density: 3 A/m$^2$).

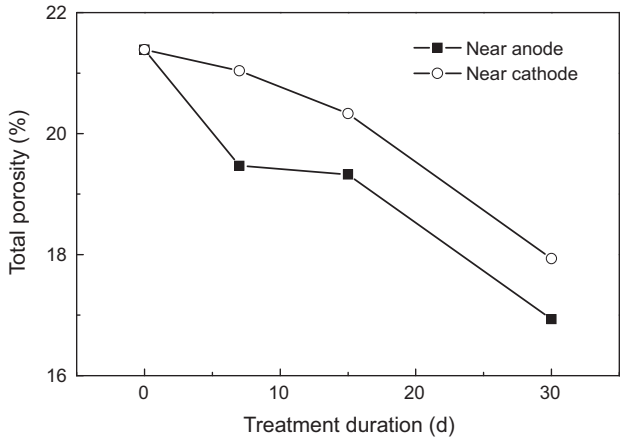


**Fig. 19.** Total porosity in concrete cover after BIEM treatment (Concrete type: 1; Mixed NaCl: 3%; Treatment duration: 0, 7, 15, 30 d; Current density: 3 A/m$^2$).

products decomposed and ions dissolved; thus, pores with small diameters appear. These ions that are soluble in concrete pore liquid will undergo directional migration under electric field action, and block some pores with large diameters during the migration process. Furthermore, in the cathodic reaction near reinforcement, water electrolysis will generate hydrogen ions whose formation of gaseous hydrogen will cause increase in porosity near the reinforcement. Thus, porosity of the concrete is higher near the cathode than near the anode.

The surface strength test indicates that after BIEM treatment, the surface strength of the concrete cover decreased. However, the mercury injection test shows that porosity on the surface of the concrete cover decreased. Hence, the application and mixing of TETA corrosion inhibitor resulted in some changes to the structure or composition of hydration products in the region near the concrete surface, which caused the strength to decrease, and the mechanism of this changing should be deeply studied in the next work. Alternatively, the dissolution, decomposition, migration, and combination with corrosion inhibitor resulted in weaker interfacial transition zone between aggregate and hydration products, leading to increase in micro-cracks.

### *4.3.2. Pore distribution variation after ECE treatment*

After ECE treatment, the porosity and pore diameter distribution in the concrete cover also changed. The porosity after ECE treatment decreased. As shown in Fig. 21, porosity of the concrete decreased when charging time increased. The reduction in porosity near the anode was more significant than that near the cathode, particularly for charging time longer than 15 days. However, ECE had a smaller effect on porosity compared with BIEM.

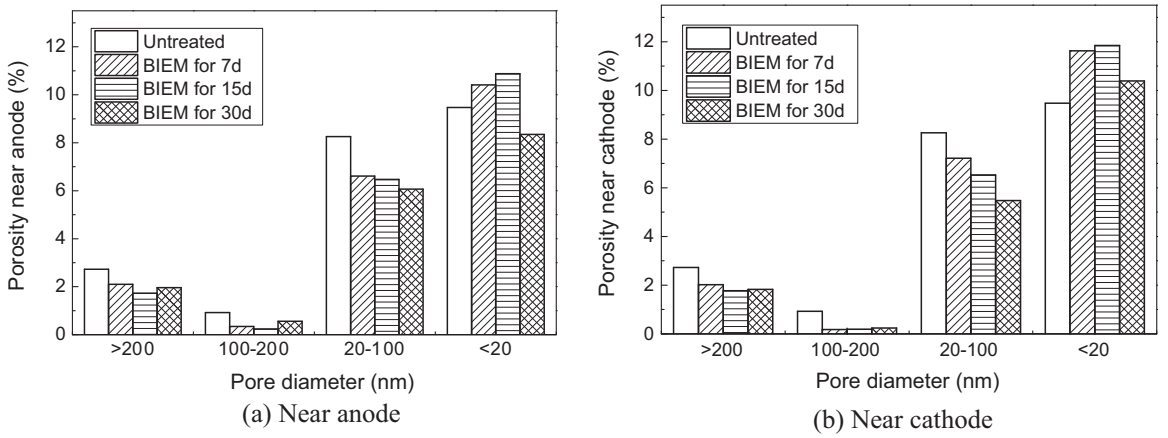


**Fig. 20.** Pore distribution in concrete cover before and after BIEM treatment (Concrete type: 1; Mixed NaCl: 3%; Treatment duration: 0, 7, 15, 30 d; Current density: 3 A/m$^2$).

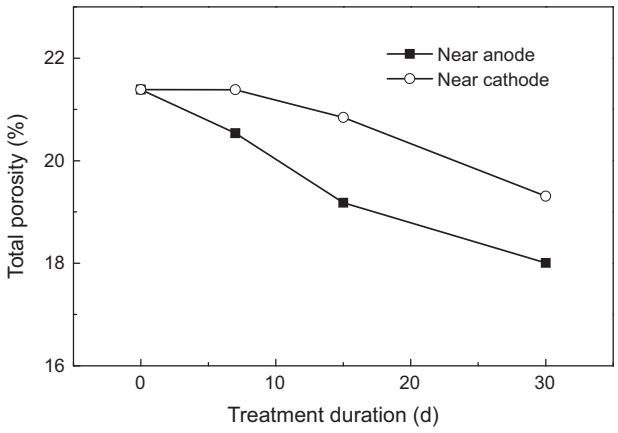


**Fig. 21.** Total porosity in concrete cover after ECE treatment (Concrete type: 1; Mixed NaCl: 3%; Treatment duration: 0, 7, 15, 30 d; Current density: 3 A/m$^2$).

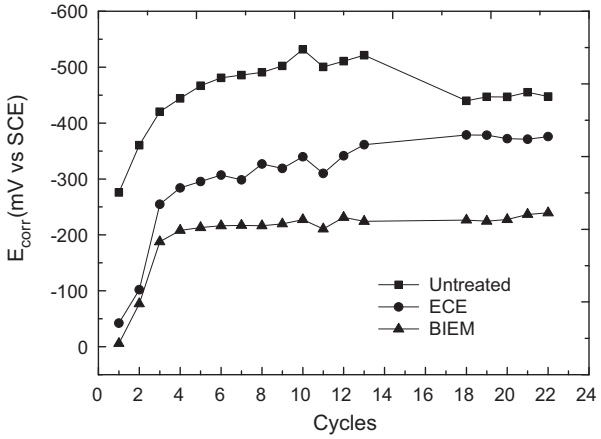


**Fig. 23.** Corrosion potential variation after drying and wetting cycles for 6 months (Concrete type: 1; Mixed NaCl: 3%; Treatment method: ECE and BIEM; Treatment duration: 15 d; Current density: 3 A/m$^2$).

Pore distribution in the concrete cover was analyzed, and the pore distribution diagrams near the anode and cathode are shown in Fig. 22. Similar to the influence of BIEM on concrete cover, the figure shows that ECE also increases small pores and reduces large pores in the concrete cover. The decreased amount of pores with little harm in a diameter of 20–100 nm was directly proportional to charging time. Harmless pores with a diameter less than 20 nm increased greatly at the initial stage of charging, and eventually increased gradually. As for the comparison between the cathode and anode, porosity of pore with great harm, pore with little harm, and harmless pore near the anode was relatively low, whereas porosity of harmful pore was high.

According to the results of the surface strength test, the process of ECE will enhance the surface strength of the concrete cover, which is consistent with porosity evolution. Thus, BIEM, by introducing TETA as corrosion inhibitor, does not generate any adverse effect on the composition and structure of hydration products near the surface of the concrete cover but instead enhances the strength of the cover compared with BIEM. Therefore, in the application of electrochemical methods to repair a concrete structure, the selection of electrolyte will result in different effects on concrete cover quality.

In conclusion, BIEM and ECE have similar influences on pore distribution in concrete cover. In general, small pores increase in number, large pores decrease in number, and total porosity decreases. However, BIEM has a greater influence on pore structure in the concrete cover and porosity reduction. Porosity reduction is more beneficial for the concrete to resist invasion by corrosive mediums such as chloride ions and oxygen. In this aspect, the concrete durability caused by BIEM is more advantageous for long-term use.

### *4.4. Long-term performance of corrosion inhibition after electrochemical repair*

#### *4.4.1. Corrosion current variation after ECE and BIEM treatment*

Normally, the corrosion potential values with more negative than −250 mV (vs SCE) can be regarded as the fact that the reinforcement is in high corrosion risk according to the ASTM standard [4]. Fig. 23 shows that the reinforcement corrosion potential of untreated test block was consistently less than −300 mV (vs SCE) , which indicates an increasing rate of reinforcement corrosion risk. The reinforcement corrosion potential of test block after ECE repair was greater than −300 mV during the first five cycles, approximately −300 mV from six to 11 cycles, and eventually less than −300 mV. Thus, reinforcement corrosion risk gradually increased. Reinforcement corrosion potential of the test block after BIEM repair decreased during the first three cycles and later almost remained unchanged between −200 and −300 mV. Thus, the possibility of reinforcement corrosion is small.

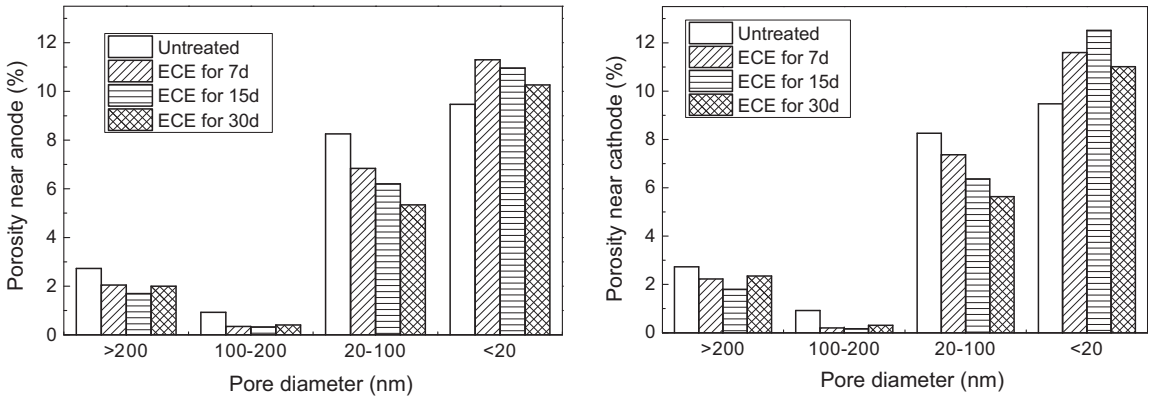


**Fig. 22.** Pore distribution in concrete cover before and after ECE treatment (Concrete type: 1; Mixed NaCl: 3%; Treatment duration: 0, 7, 15, 30 d; Current density: 3 A/m$^2$).

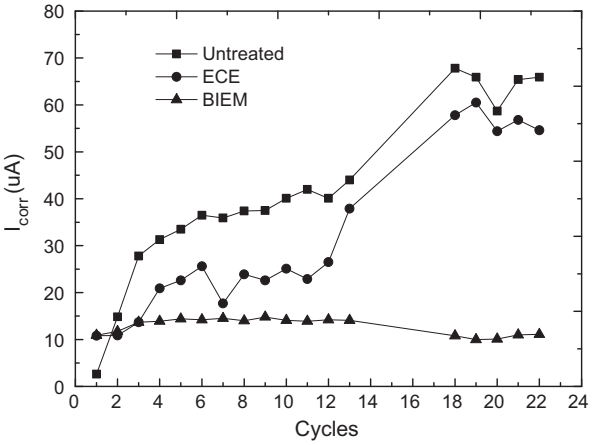


**Fig. 24.** Corrosion current variation after drying and wetting cycles for 6 months (Concrete type: 1; Mixed NaCl: 3%; Treatment method: ECE and BIEM; Treatment duration: 15 d; Current density: 3 A/m$^2$).

*4.4.2. Corrosion current variation after ECE and BIEM treatment*

Fig. 24 shows that the reinforcement of untreated test block was in a corrosion state at the beginning; during the drying and watering cycle, corrosion current increased continuously; and eventually reached 70 μA at an approximate rate of 0.62 μA/cm$^2$. This rate is significantly greater than the critical value of corrosion, 0.1–0.2 μA/cm$^2$; thus, reinforcement corrosion is quite severe [45,46]. After BIEM repair treatment, reinforcement corrosion current remained approximately 10 μA at an approximate rate of 0.09 μA/cm$^2$, which can effectively prevent secondary corrosion. However, after ECE repair, corrosion current of the test block slightly increased during the 4–11 cycles, finally reaching approximately 50 μA equaling to 0.45 μA/cm$^2$ in terms of corrosion current density. Secondary corrosion was delayed compared with the untreated test block, but severe corrosion still occurred at the end.

## 5. Conclusions

Specimens of ordinary concrete were subjected to BIEM, and the concentration profiles of $Cl^-$, $OH^-$, and corrosion inhibitor were determined in the experiment. The results showed that TETA functioned as a corrosion inhibitor, and was effectively injected into both carbonated and non-carbonated concrete investigated by relatively short-term electrochemical treatment of BIEM. The inhibitor concentration around the embedded steel reinforcement was adequate to provide corrosion protection. Moreover, the ratio of $OH^-$ to $Cl^-$ was increased because the concentration of chloride ions decreased and the concentration of hydroxyl ions was increased in the concrete cover, which favored the repassivation of reinforcement. The following conclusions can be stated:

(1) The electricity parameters should be considered in the design of the electrochemical process. The efficiencies of $Cl^-$ extraction, $OH^-$ enhancement, and TETA migration increased as the current density and/or treatment time increased during BIEM. A low current density or short treatment duration minimally affected the rehabilitation, whereas excessively high current density or excessively long treatment was unnecessary. The appropriate electricity parameters should be chosen according to the actual situation and goal of rehabilitation.
(2) The quality of the concrete also affected the electrical treatment to some degree. The efficiencies of $Cl^-$ extraction, $OH^-$ enhancement, and TETA migration decreased as the *w/c* ratio of specimens decreased. A lower *w/c* ratio signifies denser internal concrete structure and higher alkalinity, which was unfavorable for the transfer of certain particles in the electrochemical process. Thus, different electricity parameters should be chosen according to the different *w/c* ratios.
(3) Another key factor for the electrochemical process was the initial chloride content in the specimens. The specimens containing more chloride showed higher proficiency in $Cl^-$ extraction through BIEM. The alkalinity increased most in specimens mixed with 3% NaCl and increased comparatively lower in specimens mixed with 1% and 5% NaCl. The initial content of chloride in specimens had minimal influence on the migration of TETA.
(4) A significant difference was found between BIEM and ECE in the various $Cl^-$ and $OH^-$ concentrations. The residual $Cl^-$ concentration in the outer layer of the specimen was higher than the inner layer after BIEM. Nevertheless, $Cl^-$ distribution was more uniform in the specimen after ECE. The alkalinity increases in the overall concrete cover zone after the two kinds of remedial techniques only slightly differed. However, ECE was better for the alkalinity enhancement near the steel bars.
(5) The chloride-contaminated concrete structures in need of rehabilitation in on-site condition are usually carbonated to a certain depth. The migration efficiency of corrosion inhibitor in carbonated concrete was higher than non-carbonated concrete.

By contrast, LIMPET pull-out test was used to measure the surface strength of concrete samples before and after BIEM treatment. The result shows that after BIEM repair, both pull-out strength and converted compressive strength decreased. For concrete samples with charging parameters selected in this paper, the reduction range was within 10–50%. Excessive strength reduction range should be avoided in the design process for electrochemical repair schemes. By referring to research results of this paper and considering the efficiency of the TETA corrosion inhibitor, the reduction range of the surface strength can be controlled within a reasonable scope. The following conclusions can be stated:

(6) After concrete samples receive BIEM treatment, the reduction range of surface strength increases when charging time and electric current density increased. Thus, reasonable charging parameters should be selected in the practical application of BIEM.
(7) The corrosion degree of concrete caused by chloride salt has a significant effect on surface strength. For concrete samples with low initial chloride content, the reduction range of the surface strength is high. Therefore, BIEM treatment should be selected with great care in terms of reinforced concrete structure under mild chloride salt corrosion.
(8) When BIEM treatment is applied to samples after carbonization, reduction of surface strength becomes more pronounced. However, the carbonization process can generally enhance surface strength of the concrete by approximately 30%. Comprehensive analysis shows that by reasonably designing repair parameters and the repair process, surface strength reduction degree of the concrete after BIEM treatment can be controlled.
(9) Both BIEM and ECE will reduce overall porosity in the concrete cover. The porosity reduction degree of samples after BIEM treatment is higher. After BIEM and ECE treatments, pore distribution in the concrete cover changes. Harmless pores with a diameter below 20 nm increase, whereas pores with little harm, harmful pores, and pores with great harm

with a diameter greater than 20 nm decrease. Some differences are present between the concrete near the cathode and concrete near the anode in pore distribution. Porosity of concrete near the cathode is higher than that near the anode, and the specific pore distributions are also different.

(10) After BIEM treatments, chloride ion concentration on the surface of the concrete is high, whereas ECE is especially suitable for concrete surface dechlorination, which will simultaneously enhance surface strength in the concrete cover. Therefore, these two methods can be combined. Repair can be done by first adopting BIEM and later applying ECE. Thus, the damage caused by BIEM on the structure surface strength can be eliminated. Moreover, residual chloride ions in the concrete cover can be removed, which will increase repair efficiency.

## Acknowledgment

The authors would like to acknowledge the financial supports of the European Union Research Council via Grant No. 294955, the National Natural Science Foundation of PR China via Grant No. 51408534.

## References

[1] P.K. Mehta, R.W. Burrows, Building durable structures in the 21st century, Concr. Int. 23 (2001) 57–63.
[2] T. Miyagawa, Durability design and repair of concrete structures: chloride corrosion of reinforcing steel and alkali-aggregate reaction, Mag. Concr. Res. 44 (1991). 147–147.
[3] A. Djerbi, S. Bonnet, A. Khelidj, Influence of traversing crack on chloride diffusion into concrete, Cem. Concr. Res. 38 (2008) 877–883.
[4] H. Song, K.Y. Ann, S. Pack, Factors influencing chloride transport and chloride threshold level for the prediction of service life of concrete structures, Int. J. Struct. Eng. 1 (2010) 131–144.
[5] I. Martínez, C. Andrade, M. Castellote, Advancements in non-destructive control of efficiency of electrochemical repair techniques, Corros. Eng. Sci. Technol. 44 (2009) 108–118.
[6] G. Fajardo, G. Escadeillas, G. Arliguie, Electrochemical chloride extraction (ECE) from steel-reinforced concrete specimens contaminated by "artificial" seawater, Corros. Sci. 48 (2006) 110–125.
[7] J.M. Miranda, J.A. González, A. Cobo, Several questions about electrochemical rehabilitation methods for reinforced concrete structures, Corros. Sci. 48 (2006) 2172–2188.
[8] W. Yeih, J.J. Chang, C.C. Hung, Selecting an adequate procedure for the electrochemical chloride removal, Cem. Concr. Res. 36 (2006) 562–570.
[9] W. Morris, A. Vico, M. Vazquez, The performance of a migrating corrosion inhibitor suitable for reinforced concrete, J. Appl. Electrochem. 33 (2003) 1183–1189.
[10] W. Morris, M. Vázquez, A migrating corrosion inhibitor evaluated in concrete containing various contents of admixed chlorides, Cem. Concr. Res. 32 (2002) 259–267.
[11] C.K. Nmai, Multi-functional organic corrosion inhibitor, Cem. Concr. Compos. 26 (2004) 199–207.
[12] M. Ormellese, F. Bolzoni, L. Lazzari, Organic substances as inhibitors for chloride-induced corrosion in reinforced concrete, Mater. Corros. 62 (2011) 170–177.
[13] M.F. Montemor, A. Simoes, M. Ferreira, Chloride-induced corrosion on reinforcing steel: from the fundamentals to the monitoring techniques, Cem. Concr. Compos. 25 (2003) 491–502.
[14] F. Bolzoni, S. Goidanich, L. Lazzari, Corrosion inhibitors in reinforced concrete structures Part 2–Repair system, Corros. Eng. Sci. Technol. 41 (2006) 212–220.
[15] S. Sawada, C.L. Page, M.M. Page, Electrochemical injection of organic corrosion inhibitors into concrete, Corros. Sci. 47 (2005) 2063–2078.
[16] S. Sawada, J. Kubo, C.L. Page, M.M. Page, Electrochemical injection of organic corrosion inhibitors into carbonated cementitious materials: Part 1. Effects on pore solution chemistry, Corros. Sci. 49 (2007) 1186–1204.
[17] J. Kubo, S. Sawada, C.L. Page, M.M. Page, Electrochemical inhibitor injection for control of reinforcement corrosion in carbonated concrete, Mater. Corros. 59 (2008) 107–114.
[18] S.Y. Zhang, A study of corrosion inhibitors for bidirectional electromigration rehabilitation (MSc thesis), Zhejiang University, 2012.
[19] S.Y. Zhang, W.L. Jin, C. Xu, Effectiveness of an amine-based inhibitor – guanidine for steel in chloride-contaminated simulated concrete pore solutions, J. Zhejiang Univ. (Engineering Science) 47 (2013). 449-445.
[20] L.Y. Li, C.L. Page, Finite element modelling of chloride removal from concrete by an electrochemical method, Corros. Sci. 42 (2000) 2145–2165.
[21] T.D. Marcotte, C.M. Hansson, B.B. Hope, The effect of the electrochemical chloride extraction treatment on steel-reinforced mortar Part II: microstructural characterization, Cem. Concr. Res. 29 (1999) 1561–1568.
[22] M. Siegwart, J.F. Lyness, B.J. Mcfarland, Change of pore size in concrete due to electrochemical chloride extraction and possible implications for the migration of ions, Cem. Concr. Res. 33 (2003) 1211–1221.
[23] W.Z. Wang, X.M. Zheng, X.D. Liu, et al., Influence of microscopic structure in concrete by electrochemical salt releasing, Concrete 3 (2011) 8–30 (in Chinese).
[24] N.M. Ihekwaba, B.B. Hope, Mechanical properties of anodic and cathodic regions of ECE treated concrete, Cem. Concr. Res. 26 (1996) 771–780.
[25] T.A. Söylev, C. Mcnally, M.G. Richardson, The effect of a new generation surface-applied organic inhibitor on concrete properties, Cem. Concr. Compos. 29 (2007) 357–364.
[26] G. De Schutter, L. Luo, Effect of corrosion inhibiting admixtures on concrete properties, Constr. Build. Mater. 18 (2004) 483–489.
[27] Z. Heren, H. ölmez, The influence of ethanolamines on the hydration and mechanical properties of Portland cement, Cem. Concr. Res. 26 (1996) 701–705.
[28] A.E. Long, 'Improvements in or relating to strength testing brittle materials', British Standard Patent No. 1549842, Aug. 1979.
[29] Y. Bai, P. Basheer, D.J. Cleland, et al., State-of-the-art applications of the pull-off test in civil engineering, Int. J. Struct. Eng. 1 (2009) 93–103.
[30] British Standards Institution, 'Testing concrete – Part 201: Guide to the use of non-destructive methods of test for hardened concrete', BS 1881–201:1986.
[31] H.J. Ding, C. Chen, Y.X. Zhao, et al., Experimental research on the strength of concrete measured by limpet, Concrete 3 (2013) 33–36.
[32] Rakesh Kumar, B. Bhattacharjee, Assessment of permeation quality of concrete through mercury intrusion porosimetry, Cem. Concr. Res. 34 (2004) 321–328.
[33] Sidney Diamond, Mercury porosimetry, an inappropriate method for the measurement of pore size distributions in cement-based materials, Cem. Concr. Res. 30 (2000) 1517–1525.
[34] D.W. Law, J. Cairns, S.G. Millard, Measurement of loss of steel from reinforcing bars in concrete using linear polarisation resistance measurements, NDT & E Int. 37 (2004) 381–388.
[35] Luca Bertolini, Bernhard Elsener, Pietro Pedeferri, Elena Redaelli, Rob Polder, Corrosion of Steel in Concrete-Prevention, Diagnosis, Repair, Wiley-VCH, 2013, pp. 96–97.
[36] A. Eydelnant, B. Miksic, L. Gelner, Migrating corrosion inhibitors for reinforced concrete, ConChem. J. 2 (1993) 38.
[37] B. Elsener, M. Buchler, F. Stalder, Migrating corrosion inhibitor blend for reinforced concrete: part 1-prevention of corrosion, Corrosion 55 (1999) 1155–1163.
[38] L.T. Mammoliti, L.C. Brown, C.M. Hansson, The influence of surface finish of reinforcing steel and pH of the test solution on the chloride threshold concentration for corrosion initiation in synthetic pore solutions, Cem. Concr. Res. 26 (1996) 545–550.
[39] M. Castellote, C. Andrade, C. Alonso, Electrochemical removal of chlorides: modelling of the extraction, resulting profiles and determination of the efficient time of treatment, Cem. Concr. Res. 30 (2000) 615–621.
[40] S. Chatterji, On the applicability of Fick's second law to chloride ion migration through Portland cement concrete, Cem. Concr. Res. 25 (1995) 299–303.
[41] A. Costa, J. Appleton, Chloride penetration into concrete in marine environment—Part I: main parameters affecting chloride penetration, Mater. Struct. 32 (1999) 252–259.
[42] W.B. Sun, X.J. Gao, Y.Z. Yang, et al., Microstructure of concrete after electrochemical chloride extraction treatment, J. Harbin Eng. Univ. 30 (2009) 1108–1112 (in Chinese).
[43] A.J. Van Den Hondel, R.B. Polder, Electrochemical realkalisation and chloride removal of concrete, Constr. Rep. 6 (1992) 19–24.
[44] Z.W. Wu, The recent development of concrete science and technology, J. Chinese Ceram. Soc. 7 (1979) 3–7 (in Chinese).
[45] C. Alonso, M. Castellote, C. Andrade, Chloride threshold dependence of pitting potential of reinforcements, Electrochim. Acta 47 (2002) 3469–3481.
[46] C. Alonso, C. Andrade, M. Castellote, P. Castro, Chloride threshold values to depassivate reinforcing bars embedded in a standardized OPC mortar, Cem. Concr. Res. 30 (2000) 1047–1055.